ACS OMEGA

http://pubs.acs.org/journal/acsodf
Article

Experimental Study on Optimizing Hydrogen Production from Sludge by Microwave Catalytic Pyrolysis Using Response Surface Methodology

Wenchang Qin, Hailong Yu,* Chaoqian Wang, Shuting Qin, and Xiaolong Li

Cite This: ACS Omega 2024, 9, 44474−44486
Read Online

ABSTRACT: Catalytic pyrolysis technology is a harmless and useful solid waste treatment method. Studying the catalytic pyrolysis of sludge for hydrogen production is of practical significance. Therefore, this paper prepared a bifunctional catalyst with both microwave absorption and catalytic properties from electroplating sludge through carbonization and acid modification processes and then was characterized by XRD, BET, SEM, XPS, and FTIR. An experimental study employed a conventional-then-microwave pyrolysis method to investigate the catalytic pyrolysis process of municipal sludge. Combining central composite design (CCD) and response surface methodology (RSM) with three factors and five levels, this paper investigated the interactive effects of the conventional pyrolysis temperature, microwave irradiation time, and catalyst addition ratio on the unit hydrogen production (UHP) of sludge. A predictive model based on a second-order polynomial regression equation was developed. The results revealed that the catalyst possesses a specific surface area and pore structure and that the second-order polynomial model fits well. The conventional pyrolysis temperature, microwave irradiation time, catalyst addition ratio, and interaction between the latter two significantly affected the UHP of sludge. The optimal operation conditions of conventional pyrolysis temperature, microwave irradiation time, and catalyst addition ratio were 462.7 °C, 8.8 min, and 12.4%, respectively. Under these optimal conditions, the UHP was 13.22 mmol/g, with a relative error of only 1.12% compared to the predicted model value of 13.37 mmol/g.

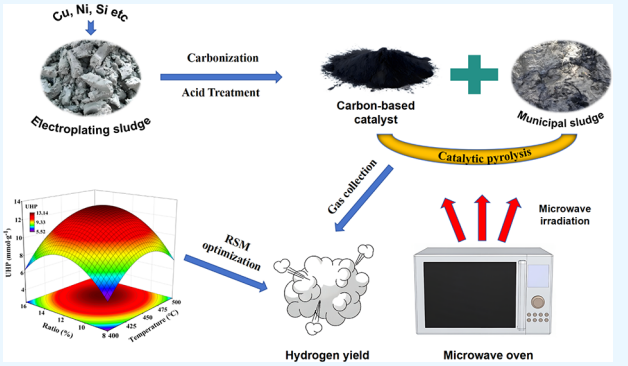

1. INTRODUCTION

Hydrogen energy, recognized globally as a clean energy source, boasts benefits such as environmental friendliness, abundant resources, and a high calorific value, holding a crucial position on the 21st-century energy stage.[1] Biomass, a renewable energy source, enjoys characteristics such as storability and transportability. Producing hydrogen from biomass has become a key focus in hydrogen energy research and utilization.[2] Recently, the increase in urban and industrial wastewater has led to a sharp rise in sewage sludge, especially municipal and electroplating sludge. This has emerged as a major environmental issue affecting sustainable socio-economic development globally.[3] Municipal sludge refers to the solid waste separated from wastewater during urban sewage treatment processes.[4] Municipal sludge contains toxic substances, including heavy metals, organic compounds, bacteria, and viruses. Studies show that these pollutants have long-term toxicity. If discharged indiscriminately, they can enter the food chain through the atmosphere, groundwater, surface water, and soil, posing severe ecological risks and affecting human health. Electroplating sludge, produced during wastewater treatment in the electroplating industry, contains heavy metals, including Cr, Ni, Cu, Zn, Hg, and Mn. These metals typically occur as mixed oxides, silicates, sulfates, or phosphates.[5] Each year, large quantities of electroplating sludge are produced globally. Japan generates around 65,000 tons,[6] the European Union 15,000 tons,[7] and China, with over 10,000 factories, produces nearly 10 million tons.[8] Electroplating sludge is categorized as hazardous waste (HW17) because of its high heavy metal content and biotoxicity.[9] If not properly treated, it can harm the environment and lead to the loss of valuable metals such as Ni, Cu, and Zn. Therefore, the proper disposal and resource utilization of sewage sludge have become critical challenges for wastewater treatment facilities. Traditional sludge disposal methods primarily include landfills, composting, and inciner-

Received: July 1, 2024
Revised: September 9, 2024
Accepted: October 16, 2024
Published: October 23, 2024

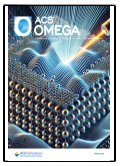

ation. Landfilling is straightforward, low-cost, and quick to implement, but it occupies a substantial amount of land and fails to utilize the resource potential of the sludge.[10] Composting improves soil structure and promotes crop growth, but it requires long fermentation times and may release toxic substances, increasing the levels of certain heavy metals in the soil.[11] Incineration rapidly reduces the sludge volume and effectively destroys pathogens. However, it can cause secondary pollution through flue gas emissions, requires significant investment in equipment, and involves complex operational procedures.[12] Currently, resource utilization is a crucial direction for sludge disposal. As a type of biomass, sludge contains substantial amounts of combustible components, such as carbon and hydrogen. Recovering and utilizing this stored energy during sludge treatment and disposal, for purposes such as gas supply, heating, or fuel substitution, can significantly improve the energy structure of China and mitigate environmental issues in China. Additionally, sludge contains substantial organic matter, which can be used for hydrogen production. Current methods for producing hydrogen from sludge include biological fermentation, gasification, and pyrolysis.[13] Pyrolysis technology, known for its energy-saving and eco-friendly merits, is gaining attention for producing hydrogen-rich gas and resourceful waste disposal.[14] Sludge pyrolysis technology involves heating sludge to decompose organic matter under anaerobic or anoxic conditions, producing bio-oil, biogas, and carbon residues. Compared with other methods, sludge pyrolysis recovers high-quality hydrogen-rich gas and minimizes secondary pollution. It is an efficient, eco-friendly, and economically viable technology for hydrogen production.

Microwaves are electromagnetic waves with frequencies ranging from 300 MHz to 300 GHz. Microwave heating occurs when a material absorbs microwave energy, converting it into thermal energy and raising the material's macroscopic temperature.[15] The primary heating mechanisms are dielectric loss, hysteresis loss, and resistive loss.[16] Due to its selective, rapid, and uniform heating with strong penetration,[17] microwave pyrolysis technology shows significant potential for treating solid wastes like sludge. Compared to conventional pyrolysis technology, microwave pyrolysis requires shorter heating times, consumes less energy, and is easier to control.[18] Furthermore, studies shown that microwave technology achieves higher hydrogen yields in sludge pyrolysis than conventional methods.[19] For example, Dominguez et al. conducted experiments using microwave pyrolysis and traditional electric heating on sludge. Their results showed that microwave pyrolysis produced higher concentrations of H_2 and CO.[20] Similarly, Liu et al. designed a microwave pyrolysis setup to pyrolyze the sludge. They found that higher final pyrolysis temperatures resulted in higher gas yields, with increased H_2 and CO content.[21] Using optimal conditions from their experiments, they conducted continuous high-temperature microwave pyrolysis, achieving a combined H_2 and CO volume fraction of up to 67%.

Temperature, residence time, and catalysts are crucial factors affecting hydrogen production from sludge via microwave pyrolysis.[22] Fuentes-Cano et al. analyzed gas characteristics from sludge pyrolysis and found that H_2 is mainly released at around 450 and 700 °C, with the highest H_2 content at approximately 1000 °C.[23] Since sludge is a weak microwave absorber, achieving high temperatures requires either adding significant amounts of strong microwave absorbers or increasing microwave energy consumption.[24] Yu et al. found that without activated carbon, irradiating 30 g of wet sludge (76.8% moisture content) at 700 W for 60 min raised the maximum temperature to only 149 °C.[25] Wang et al. discovered that regardless of the microwave absorber, the initial stage of microwave irradiation of wet sludge involves dehydration. When dry sludge is irradiated in a microwave, its maximum temperature reaches only about 337 °C.[26] Consequently, many researchers have added effective microwave absorbers like activated carbon, SiC, and graphite to increase sludge temperature during microwave pyrolysis for gas production. Residence time is the duration for which a sample stays at the target pyrolysis temperature. It significantly influences the composition and yield of gases produced from sludge pyrolysis. Liu et al. investigated the microwave pyrolysis of 4 kg of wet sludge, containing 81.9% moisture, using 1600 W microwave power and reaching a final temperature of 800 °C. They examined the effects of residence times of 30, 40, 50, 60, and 70 min on gas production. The results showed that the gas yield increased with longer residence times. The highest H_2 content and maximum H_2 yield were observed at 50 min.[21] Additionally, catalysts are crucial in hydrogen production from sludge through microwave pyrolysis, accelerating the conversion of specific active components into hydrogen.[27] Lin et al. examined the impact of five catalysts (H_3PO_4, H_3BO_3, KOH, $ZnCl_2$, and $FeSO_4$) on the syngas yield from microwave-assisted sludge pyrolysis. Results indicated that adding $FeSO_4$ and $ZnCl_2$ increased the syngas yield by 8.5% and 13.2%, respectively, demonstrating their catalytic effect on the pyrolysis of organic matter in sludge.[28] Chen et al. investigated the effects of different catalysts on biogas release from microwave sludge pyrolysis. Their results indicated that nickel-based catalysts had the best catalytic effect on gas production. A 5% catalyst addition at a final pyrolysis temperature of 800 °C yielded the highest H_2 and CO production, increasing H_2 yield by 23.4%.[29] However, scaling up sludge treatment with increased microwave-absorbing media and catalysts can significantly raise practical application costs. Additionally, issues like catalyst deactivation and postpyrolysis separation difficulties further complicate sludge treatment.[30]

In recent years, carbon-based catalysts have been widely applied in microwave catalytic pyrolysis. They typically possess large specific surface areas and rich pore structures. During biomass pyrolysis, these catalysts can enhance reaction rates by catalyzing active components, resulting in more high-value products.[31] An et al. studied the catalytic reforming of palm kernel shell pyrolysis vapors using Fe-loaded carbon-based catalysts, finding a 36.13% increase in H_2 content by volume.[32] Dong et al. discovered that Fe-modified carbon-based catalysts facilitated the pyrolysis of moso bamboo, producing large amounts of CO and H_2. The gaseous phase had a significantly higher calorific value than typical biomass gasification fuels.[33] Some researchers have directly converted carbon residues from pyrolysis into catalysts through post-treatment. This method reduces dependence on external raw materials, lowers environmental pollution from waste disposal, and aligns with green and circular economy principles. Electroplating sludge contains a variety of heavy metals that act as active centers in catalytic reactions, accelerating the chemical processes. For instance, Ni and Cu are commonly used catalysts, widely applied in the pyrolysis of organic compounds and gas reforming.[34] Heavy metal catalysts facilitate the breakdown

https://doi.org/10.1021/acsomega.4c06104
ACS Omega 2024, 9, 44474−44486

Table 1. Ultimate and Proximate Analysis of Municipal Sludge

Proximate analysis w/% (dry basis)				Ultimate analysis w/% (dry basis)				
M_{ad}	A_{ad}	V_{ad}	FC_{ad}	C	H	O	N	S
5.36	55.94	32.93	5.77	34.17	5.89	12.54	4.97	1.63

of hydrocarbons during pyrolysis, thereby increasing the hydrogen production rates. Carbonization of electroplating sludge produces carbon-based materials that are enriched with heavy metals. These materials possess high surface areas and abundant pore structures that enhance the catalytic performance. In microwave-assisted pyrolysis, the combination of heavy metals and carbon-based materials more efficiently absorbs microwave energy, converting it into heat, thus, accelerating the reaction. Furthermore, electroplating sludge is a hazardous waste. Using it as a catalyst not only allows for resource recovery and reduces material costs but also mitigates its environmental impact, aligning with green chemistry and circular economy principles.

Currently, many reports address the factors affecting the production of hydrogen from sludge pyrolysis. However, the simultaneous effects of multiple factors on hydrogen production and the optimal levels of these factors remain unclear. Fortunately, a full factorial experiment can address this issue but it is time-consuming and labor-intensive. Therefore, a statistical method is needed to overcome this drawback. Response surface methodology (RSM) is a statistical tool originating from experimental design, later introduced into numerical simulation for reliability assessment of complex multivariable systems.[35] Compared with other statistical methods, RSM accurately estimates the relationship between the response and key factors near the optimum. It also determines the optimal conditions using a second-order polynomial model.[36] Generally, RSM's experimental design methods include central composite design (CCD) and Box–Behnken design. When combined with CCD, RSM offers a wider range for finding optimal conditions compared to other designs.[37] To date, numerous studies have focused on the hydrogen yield from microwave catalytic pyrolysis of sludge. However, few studies have reported on using carbon-based catalysts derived from sludge for pyrolysis to produce hydrogen. Additionally, the application of RSM to study the simultaneous effects of multiple factors on the production of hydrogen from sludge pyrolysis is lacking.

Therefore, without any additional media, we prepared and characterized a bifunctional carbon-based catalyst from electroplating sludge, which possessed both microwave absorption and catalytic properties. The experiment was divided into two phases to increase the temperature for hydrogen production from sludge pyrolysis. First, partial pyrolysis of sludge was performed through short-term, low-temperature conventional pyrolysis, moderately enhancing and adjusting its dielectric properties and microwave heating characteristics. Second, the initially pyrolyzed sludge underwent microwave catalytic pyrolysis using microwave heating.[38] We specifically investigated the effects of the conventional pyrolysis temperature, microwave irradiation time, and catalyst addition ratio on the unit hydrogen production (UHP) of sludge during microwave pyrolysis. Through response surface methodology (RSM), we sought optimal conditions for hydrogen production.

2. EXPERIMENT SECTION

2.1. Experimental Materials and Reagents. This experiment involved two types of sludge: municipal sludge and electroplating sludge (primarily composed of Ni and Cu), both sourced from a sewage treatment plant in Changzhou. The elemental and proximate analyses of municipal sludge are shown in Table 1. Table 2 presents the physicochemical properties of the electroplating sludge. Both samples were sun-dried for 1 week, then placed in an oven at 105 °C and dried for 48 h to a constant weight. The dried sludge blocks were crushed using a grinder and sieved through a 20-mesh screen. The collected samples were stored in sealed bags for later use. The reagents used included HNO_3 (analytical grade, Sinopharm Group), deionized water (analytical grade, Suzhou Aiying), and Sesbania powder (industrial grade, Shandong Siyang).

Table 2. Physicochemical Properties of Electroplating Sludge

Proximate analysis w/% (dry basis)		Metal element analysis w/% (dry basis)	
M_{ad}	7.45	Cr	1.3
A_{ad}	63.21	Ni	9.5
V_{ad}	23.55	Cu	10.8
FC_{ad}	5.79	Si	1.6
–	–	Al	0.4
Mineral composition w/% (dry basis)			
Cu_2O	11.42	Fe_2O_3	2.41
SiO_2	1.32	NiO	8.75
CrO_3	0.17	Al_2O_3	0.39
CaO	0.04	ZnO	0.01

2.2. Catalyst Preparation. Catalyst samples were prepared from electroplating sludge through processes, including carbonization and nitric acid modification.[39] The preparation method is as follows: first, Sesbania powder (5% mass fraction) was mixed thoroughly with electroplating sludge and then HNO_3 solution (1% mass fraction). The mixture was extruded into strips and dried at 110 °C for 4 h. Subsequently, the dried strips were roasted in a tubular furnace at 600 °C for 3 h under a nitrogen (N_2) atmosphere. This process produces carbonized electroplating sludge, labeled as SC (precursor catalyst). To enhance its pore structure, specific surface area, and reactivity,[40] an acid modification was performed on SC. 3 g of carbonized electroplating sludge was submerged in 12 mL of 5 mol/L HNO_3 solution. The sample was incubated in a sealed bottle at 0 °C for 24 h. The modified SC was rinsed with deionized water until the pH is neutral. Finally, it was dried in an oven at 110 °C for 3 h to obtain the HNO_3-modified sludge carbon catalyst, labeled as SC-M.

2.3. Catalyst Characterization. The phase composition and crystalline structure changes of SC-M were analyzed by using an X-ray powder diffractometer (D/MAX2500, Rigaku, Japan). The test conditions included a scanning speed of 2°/min, a scanning range of 10–90°, and an X-ray source with a copper target. A physical adsorption instrument (Autosorb-

https://doi.org/10.1021/acsomega.4c06104
ACS Omega 2024, 9, 44474–44486

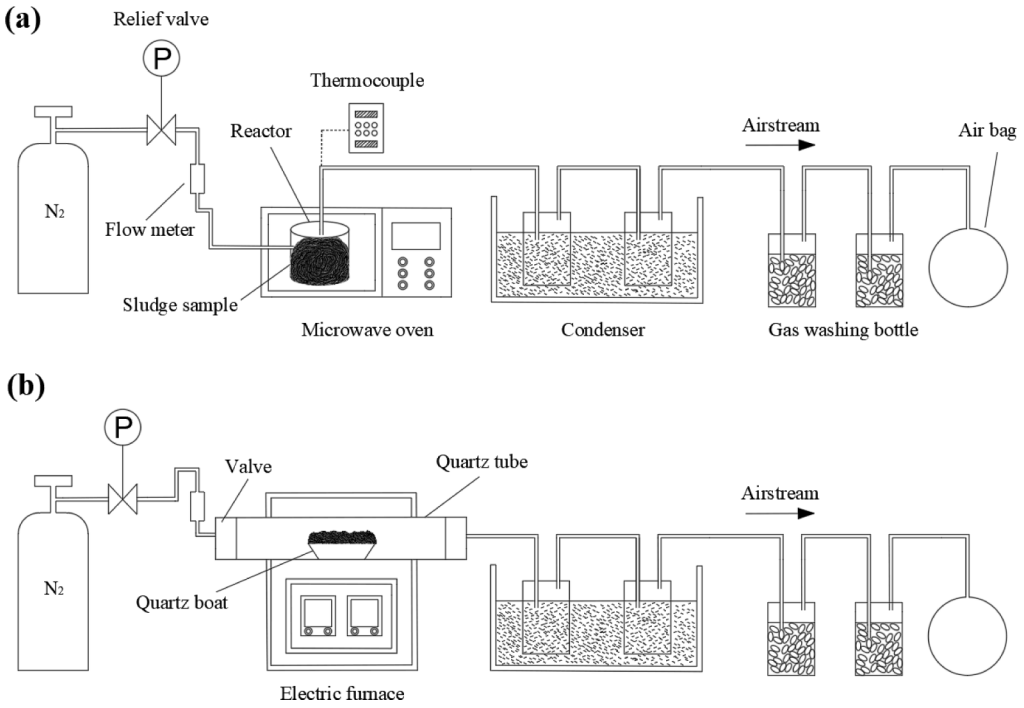

Figure 1. Diagram of (a) the microwave pyrolysis device and (b) the conventional pyrolysis device.

IQ2-MP, Quantachrome Instruments, USA) was used to test the nitrogen adsorption and desorption of SC-M at 77K liquid nitrogen. The sample's specific surface area and pore characteristics were analyzed. The microstructure of SC-M was observed using a field emission scanning electron microscope (SUPRA55, Zeiss, Germany) at magnifications ranging from 944 to 10,000 times. The chemical composition, elemental content, and oxidation states of SC-M were analyzed by X-ray photoelectron spectroscopy (ESCALAB250XI, Thermo Fisher Scientific, USA). Surface functional groups of SC-M were identified by Fourier Transform Infrared spectroscopy (Nicolet 6700, Thermo Fisher, USA). A DTGS detector was used, operating within a wavenumber range of 400−4000 cm^{-1} and a resolution of 4 cm^{-1}.

2.4. Experimental Apparatus and Operation Method. The schematic diagram of our pyrolysis apparatus is shown in Figure 1. (a) Microwave heating device (EMA34GTQ-SS, Changzhou Huari Electric Appliance Company) operates at a frequency of 2450 MHz with a rated power of 1200 W. (b) The tube electric heating furnace (HWL-10GKQ, Shandong Huawei Furnace Industry Company) has a rated power of 5 kW and a heating range of 0−1200 °C. It is equipped with an intelligent temperature control system.

In the initial routine pyrolysis experiment, a specific mass of municipal sludge was placed in a quartz boat. The nitrogen cylinder valve was opened to purge the system for 10 min to remove air. The tube furnace was then heated to a predetermined temperature at a rate of 20 °C/min. The quartz boat was sent to the center of the heating tube using a push rod, and the feed end of the heating tube was sealed with a valve. Nitrogen (N_2) was introduced into the pyrolysis system at a rate of 150 mL/min. The pyrolysis time was set to 20 min. In the microwave pyrolysis experiment, the microwave power was consistently set to 1200 W. 20 g portion of preliminarily pyrolyzed sludge was placed in a quartz reactor, and a corresponding proportion of SC-M catalyst was added based on the mass of 20 g of sludge. After setting the microwave irradiation time and fully pyrolyzing, the collected biogas was introduced into a gas chromatograph (FP6890, Hewlett-Packard, USA) to determine the H_2 concentration. The UHP from sludge pyrolysis was calculated as follows: first, the volume of H_2 was obtained by multiplying the gas yield by the H_2 volume content. Then, the volume of H_2 at standard conditions (0 °C, 101.325KPa) was calculated under the ideal gas equation $PV = nRT$. From this, the molar amount of H_2 (n) was calculated using eq 1. Finally, the UHP (Y) was calculated by using eq 2.

$$n = \frac{V}{22.4} \tag{1}$$

$$Y = \frac{n \times 1000}{m} \tag{2}$$

Here, n represents the molar amount of hydrogen, V is the volume of hydrogen at standard conditions, m is the mass of the sludge (20 g), and Y is the unit hydrogen production.

2.5. Experiment Design. *2.5.1. Single-Factor Experiment.* (1) Effect of conventional pyrolysis temperature on UHP. The effect of conventional pyrolysis temperatures of 375 °C, 400 °C, 425 °C, 450 °C, 475 °C, 500 °C, and 525 °C on the UHP from sludge pyrolysis was investigated under a microwave irradiation time of 8 min and a catalyst addition ratio of 12%.

(2) Effect of microwave irradiation time on UHP. The effect of microwave irradiation times of 2, 4, 6, 8, 10, 12, and 14 min on the UHP from sludge pyrolysis was investigated under a conventional pyrolysis temperature of 450 °C and a catalyst addition ratio of 12%.

(3) Effect of catalyst addition ratio on UHP. The effect of catalyst addition ratios of 6%, 8%, 10%, 12%, 14%, 16%, and 18% on the UHP from sludge pyrolysis was investigated under

https://doi.org/10.1021/acsomega.4c06104
ACS Omega 2024, 9, 44474−44486

a conventional pyrolysis temperature of 450 °C and a microwave irradiation time of 8 min.

2.5.2. Response Surface Experiment. A central composite design (CCD) was used, with X_1 (conventional pyrolysis temperature), X_2 (microwave irradiation time), and X_3 (catalyst addition ratio) as independent variables and y (UHP) as the dependent variable. Based on single factor test results, a 3-factor, 5-level design was selected. The specific factors and levels are shown in Table 3. A regression analysis

Table 3. Factors and Levels in the Experiment

Independent variables	Coded variable levels				
	−2	−1	0	1	2
microwave irradiation time/min	4	6	8	10	12
conventional pyrolysis temperature/°C	400	425	450	475	500
catalyst addition ratio/%	8	10	12	14	16

was conducted on the experimental data using Design Expert software. The quadratic polynomial mathematical model is expressed in eq 3:

$$y = \beta_0 + \sum_{i=1}^{n} \beta_i X_i + \sum_{i=1}^{n} \beta_{ii} X_i^2 + \sum_{i<j}^{n} \beta_{ij} X_i X_j \quad (3)$$

where y represents the predicted unit hydrogen production value, X_i and X_j are independent variables, β_0 is a constant, β_i, β_{ii}, and β_{ij} are the parameters of linear, interaction term, and quadratic terms, respectively,[41] which need to be fitted. The design consisted of 5 center points and a star arm length of 2, totaling 19 experiments to complete the optimization. All experiments were conducted randomly to minimize external interference with the results. Table 4 presents the design and results of the experiments.

3. RESULTS AND DISCUSSION

3.1. Characterization of SC-M Catalyst. *3.1.1. X-Ray Powder Diffraction Analysis.* Figure 2 displays the XRD pattern of the SC-M catalyst. The SC-M catalyst exhibits

Table 4. Response Surface Test Design and Results

Run	X_1/°C	X_2/min	X_3/%	y/mmol g^{-1}
1	425	6	10	8.49
2	475	6	10	9.04
3	450	8	12	12.84
4	425	6	14	9.77
5	450	4	12	8.15
6	475	6	14	10.86
7	450	8	12	13.17
8	400	8	12	9.16
9	450	8	16	10.91
10	425	10	10	10.55
11	425	10	14	10.62
12	450	8	12	13.23
13	500	8	12	11.94
14	475	10	10	11.70
15	475	10	14	12.10
16	450	12	12	10.74
17	450	8	8	9.40
18	450	8	12	12.98
19	450	8	12	13.17

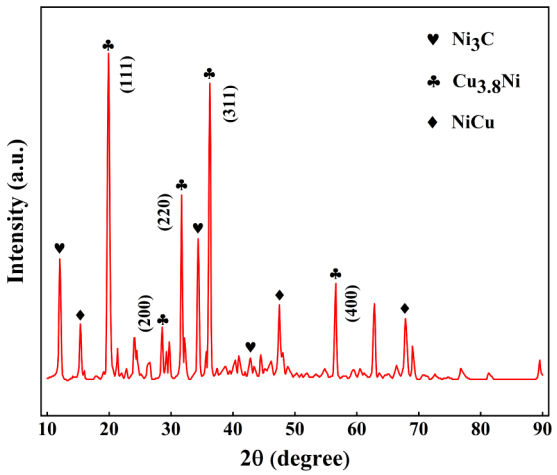

Figure 2. XRD spectra of the SC-M catalyst.

characteristic diffraction peaks ranging from 12.4° to 67.8°. By comparison with the database, the diffraction peaks at 19.9°, 28.6°, 31.7°, 36.3°, and 56.6° were identified as corresponding to $Cu_{3.8}Ni$, a primary crystal structure matching the standard card (PDF: 09-0205). These peaks correspond to the (111), (200), (220), (311), and (400) planes of Cu3.8Ni. The remaining diffraction peaks correspond to NiCu and Ni_3C, potentially serving as the main active sites. Due to the likely small particle size undetectable by the X-ray diffractometer,[42] characteristic diffraction peaks of NiO_x and Cu_xO were not observed.

3.1.2. Surface Property Analysis. Figure 3a shows the N_2 adsorption−desorption isotherm curves of the SC-M catalyst. These curves, within a relative pressure range of 0−1, align with type IV isotherms and exhibit H3-type hysteresis loops. It is suggested that SC-M may have large voids or cracks between the plate-like particles or within pores. Figure 3b shows the BJH pore size distribution of the SC-M catalyst. The average pore size was logarithmically processed for easier observation of data points. The pore size distribution of SC-M ranges from 2 to 100 nm, with a higher concentration of pores in the 2−20 nm range. This indicates that the SC-M catalyst is a mesoporous material. Additionally, the pore size distribution of SC-M shows a bimodal or multimodal structure, suggesting the existence of a hierarchical pore system. This hierarchical structure enhances the performance of SC-M.

Table 5 summarizes the physicochemical properties of the SC-M catalyst. It shows that the catalyst possesses a specific surface area and pore structure.

3.1.3. Scanning Electron Microscopy Analysis. Figure 4 shows the scanning electron microscopy (SEM) images of the SC-M catalyst at different magnifications. These images indicate that the catalyst primarily consists of pores of various sizes and dense agglomerates of irregular particles. The surface exhibits a distinct porous structure.

3.1.4. X-ray Photoelectron Spectroscopy Analysis. The XPS spectra of the SC-M catalyst are shown in Figure 5. According to Figure 5a, the SC-M catalyst contains Ni, Cu, C, O, and Si. The C 1s spectrum of SC-M is deconvoluted into three distinct peaks: C═O (288.2 eV), C−C (284.6 eV), and sp^2 C (283.8 eV), indicating the presence of carbon layers within the SC-M catalyst (Figure 5b).[43] The Cu 2p XPS spectrum of the SC-M catalyst is presented in Figure 5c. Peaks at 931.7 and 952.1 eV are attributed to Cu^+ in the Cu $2p_{3/2}$

https://doi.org/10.1021/acsomega.4c06104
ACS Omega 2024, 9, 44474−44486

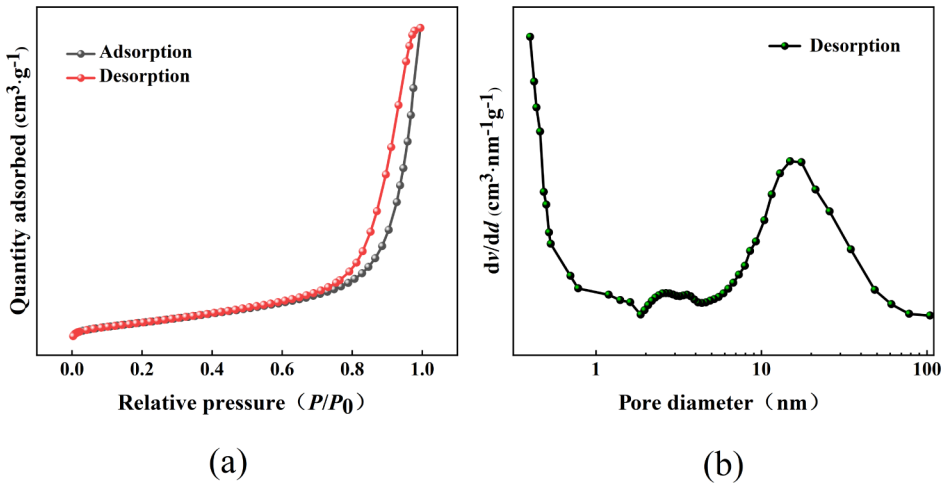

Figure 3. (a) N_2 adsorption desorption isotherms of the SC-M catalyst; (b) BJH pore size distribution curve for the SC-M catalyst.

Table 5. Physical and Chemical Properties of the SC-M Catalyst

Catalyst	Specific surface area/ ($m^2 \cdot g^{-1}$)	Pore volume / ($cm^3 \cdot g^{-1}$)	Average pore size/ (nm)
SC-M	24.8	0.1062	14.68

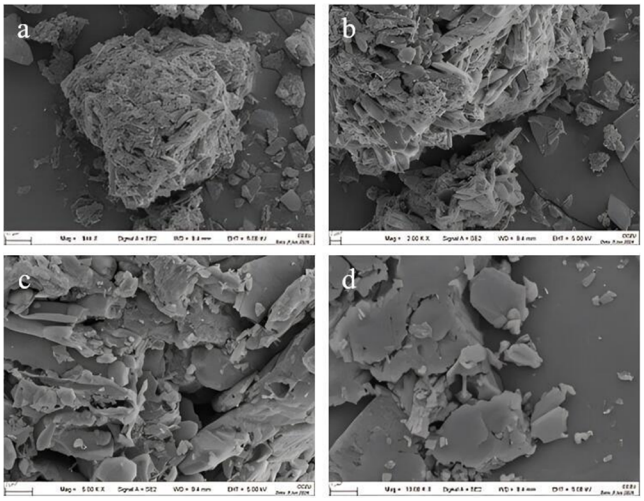

Figure 4. SEM images of the SC-M catalyst (a: 944×, b: 2000×, c: 5000×, d: 10,000×).

and Cu $2p_{1/2}$ states, respectively, confirming the presence of Cu_2O within the catalyst.[44] Peaks at 933.4 and 954.0 eV correspond to Cu^{2+} in the Cu $2p_{3/2}$ and Cu $2p_{1/2}$ states, indicating the presence of CuO. Additionally, three satellite peaks at binding energies of 961.8, 943.2, and 941.1 eV correspond to the Cu^{2+} state of Cu atoms.[45] The Ni 2p XPS spectrum of the SC-M catalyst is depicted in Figure 5d. Peaks at 872.6 and 855.1 eV are linked to Ni^{2+}, while fitted peaks near 873.5 and 856.2 eV are ascribed to Ni^{3+}.[46] Furthermore, peaks at 879.6 and 861.0 eV on the high binding energy side of the Ni $2p_{1/2}$ and Ni $2p_{3/2}$ edges are identified as satellite peaks of Ni.

3.1.5. Fourier Transform Infrared Spectroscopy Analysis. Figure 6 shows the FTIR spectrum of the SC-M catalyst. The peak at 1617 cm^{-1} corresponds to a C═C bond, indicating aromatic rings or alkenes within SC-M.[47] Smaller peaks at 1105 and 1231 cm^{-1} correspond to C−H bonds. Distinct peaks at 684 and 503 cm^{-1} are linked to Cu−O and Ni−O groups, respectively.[48] Cu−O and Ni−O suggest that copper and nickel are primarily in oxidized forms, as confirmed by Cu_2O and NiO in Table 2. Ni−O bonds act as active sites in catalytic reactions, enhancing the selectivity and stability of SC-M. Cu−O exhibits strong electron transfer capabilities, facilitating reactant activation and enhancing the overall activity of SC-M. Peaks at 3433 and 2926 cm^{-1} correspond to −OH groups from alcohols and phenols and −COOH groups from carboxylic acids and their derivatives.[49] Additionally, the Si−O−Si group detected at 1105 cm^{-1} indicates the presence of SiO_2 in SC-M. SiO_2 provides thermal stability and mechanical strength, increasing the surface area of SC-M and thereby enhancing the catalytic efficiency.

3.2. Single-Factor Experiment Results. *3.2.1. Effect of Conventional Pyrolysis Temperature on UHP.* As shown in Figure 7a, the UHP initially increases and then decreases as the conventional pyrolysis temperature rises. The UHP values at 400 and 500 °C are similar. At 450 °C, UHP reaches its peak value of 12.03 mmol/g. Table 6 displays the gas composition at different conventional pyrolysis temperatures. As the temperature increases from 375 to 450 °C, H_2 content rises from 12.48% to 26.46%, while the CO content grows from 13.51% to 25.53%. In contrast, the CO_2 content decreases from 36.33% to 26.54%, and the CH_4 content drops from 18.76% to 12.09%. The reaction (eq 4) between CH_4 and CO_2 at elevated temperatures likely contributes to the increased production of H_2 and CO.

$$CH_4 + CO_2 \rightarrow 2CO + 2H_2 \quad \Delta H_{298\,K} = 247.9\ kJ/mol \tag{4}$$

However, further increases in pyrolysis temperature lead to a decline in H_2 content, dropping to 22.75% at 525 °C. This reduction may result from secondary reactions, such as

$$CO + 3H_2 \rightarrow CH_4 + H_2O \quad \Delta H_{298\,K} = -206.1\ kJ/mol \tag{5}$$

methanation (eq 5),[50] that reduce H_2 yield. The gradual increase in CH_4 content above 450 °C supports this hypothesis. Thus, temperatures of 400 °C, 425 °C, 450 °C, 475 °C, and 500 °C were selected for the optimization experiment.

3.2.2. Effect of Microwave Irradiation Time on UHP. As shown in Figure 7b, the UHP increases gradually up to 8 min

https://doi.org/10.1021/acsomega.4c06104
ACS Omega 2024, 9, 44474−44486

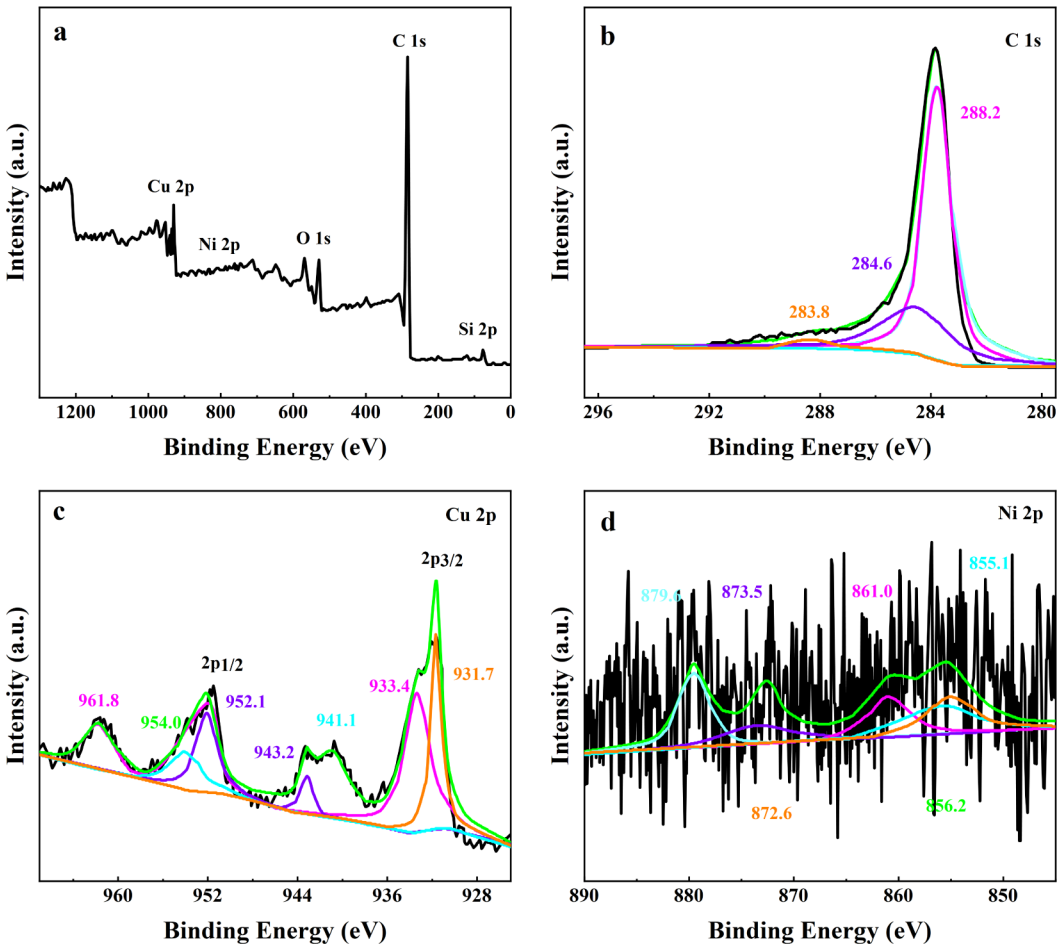

Figure 5. (a) XPS spectra of the SC-M catalyst; (b) XPS of C 1s over the SC-M catalyst; (c) XPS of Cu 2p over the SC-M catalyst; (d) XPS of Ni 2p over the SC-M catalyst.

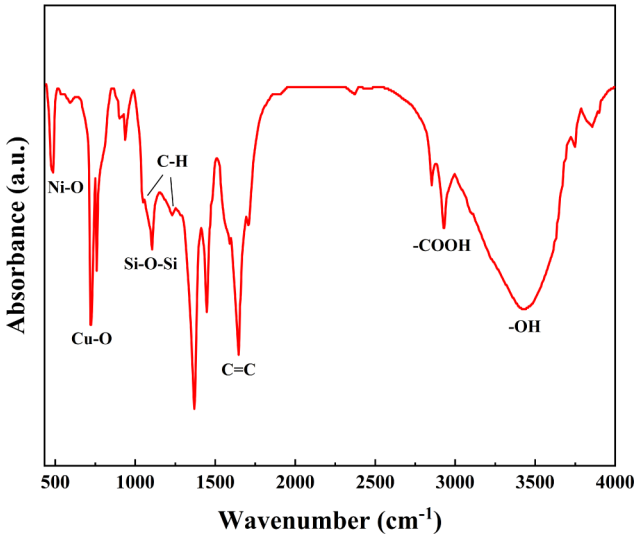

Figure 6. FTIR spectra of the SC-M catalyst.

of microwave irradiation time and then decreases significantly. This decrease is likely due to high temperatures from prolonged irradiation, which intensifies the reaction, causing undecomposed organic matter and small molecules to escape the pyrolysis system with the generated gas, thus reducing hydrogen production. Table 7 shows that the total content of H_2 and CO increases from 17.77% at 2 min to 49.02% at 8 min, while the combined content of CH_4 and CO_2 decreases from 56.17% to 35.25%. Two key factors explain this trend. First, CH_4 and CO_2 are converted into H_2 and CO through the reaction (eq 4).

Second, carbon produced during pyrolysis reacts (eq 6) with CO_2 at high temperatures,[51] while the thermal decomposition of CH_4 (eq 7) further increases H_2 yield.[52] Moreover, microwaves induce a hotspot effect, forming localized high-temperature zones within the sludge. These hotspots significantly accelerate reaction rates and promote

$$C(s) + CO_2 \rightarrow 2CO \quad \Delta H_{298\,K} = 173\ kJ/mol \tag{6}$$

$$CH_4 \rightarrow C(s) + 2H_2 \quad \Delta H_{298\,K} = 75.6\ kJ/mol \tag{7}$$

rapid organic decomposition.[53] Prolonging the microwave irradiation time further amplifies the hotspot effect, resulting in higher H_2 yield. However, excessive irradiation time may cause carbonization or charring, potentially impeding the reaction process and ultimately reducing the H_2 yield. Therefore, irradiation times of 4, 6, 8, 10, and 12 min were chosen for the optimization experiment.

3.2.3. Effect of Catalyst Addition Ratio on UHP. As illustrated in Figure 7c, under constant conditions, the UHP increases when the catalyst addition ratio ranges from 6% to 12%. However, when the ratio exceeds 12%, the UHP begins to decrease. This decrease is likely due to an excessive catalyst

https://doi.org/10.1021/acsomega.4c06104
ACS Omega 2024, 9, 44474−44486

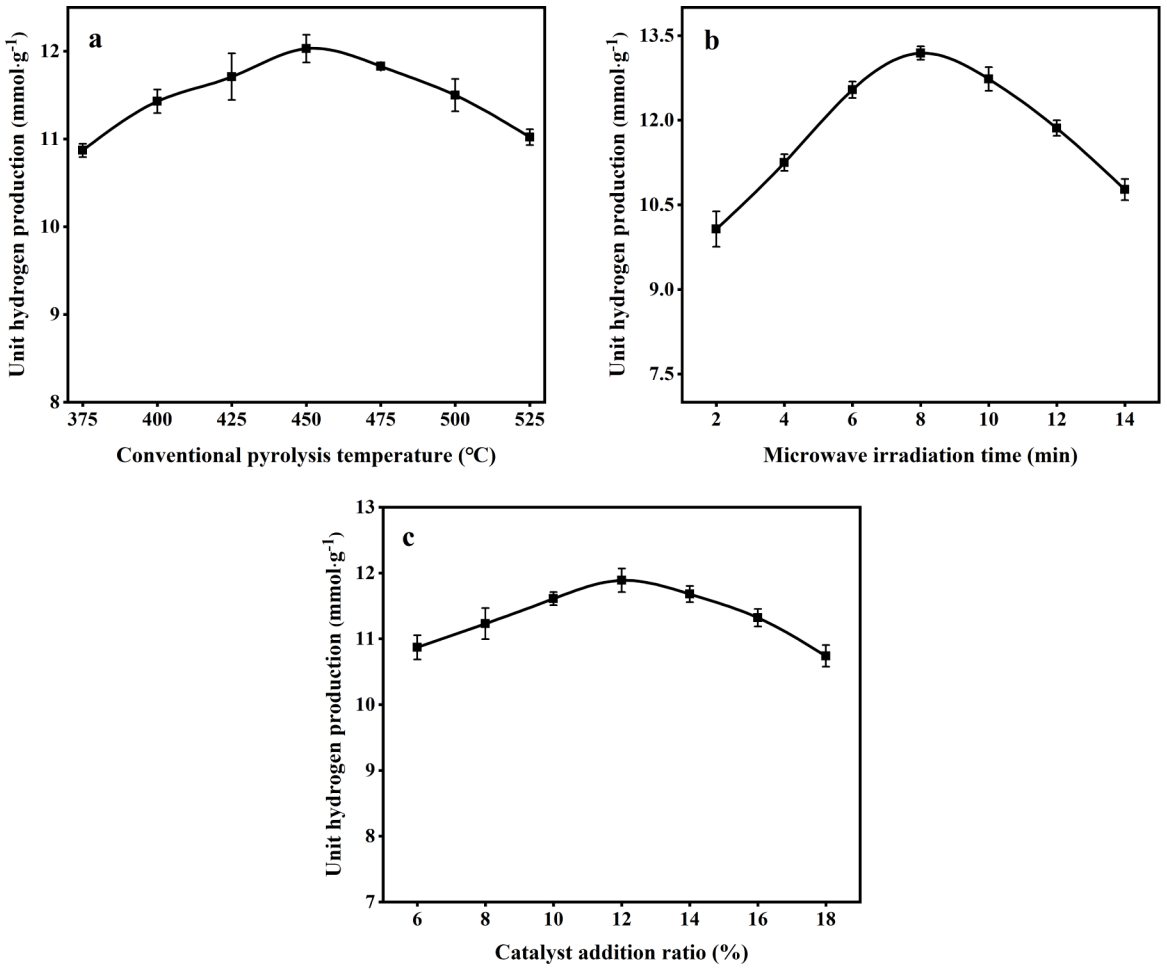

Figure 7. Effect of single factors on UHP: (a) conventional pyrolysis temperature; (b) microwave irradiation time; (c) catalyst addition ratio.

Table 6. Gas Composition at Different Conventional Pyrolysis Temperatures

Conventional pyrolysis temperature (°C)[a]	H_2 (%)	CO (%)	CO_2 (%)	CH_4 (%)	C_xH_y (%)
375	12.48	13.51	36.33	18.76	18.92
400	15.65	14.72	32.27	16.43	20.93
425	18.85	16.04	28.48	15.02	21.61
450	26.46	25.53	26.54	12.09	9.38
475	23.23	22.19	27.42	12.98	14.18
500	22.80	23.57	28.28	13.56	11.79
525	22.75	22.46	29.74	13.77	11.28

[a]Conditions: microwave irradiation time of 8 min and catalyst addition ratio of 12%.

Table 7. Gas Composition at Different Microwave Irradiation Times

Microwave irradiation time (min)[a]	H_2 (%)	CO (%)	CO_2 (%)	CH_4 (%)	C_xH_y (%)
2	8.45	9.32	38.52	17.65	26.06
4	10.33	12.46	36.31	16.24	24.66
6	17.95	15.82	33.67	14.81	17.75
8	29.68	19.34	24.71	10.55	15.72
10	28.57	17.51	25.32	12.48	16.12
12	27.43	18.66	27.90	13.15	12.86
14	27.18	17.53	28.44	12.76	14.09

[a]Conditions: conventional pyrolysis temperature of 450 °C and catalyst addition ratio of 12%.

content causing carbon deposits from decomposition and polymerization reactions. These deposits further reduce the catalyst's specific surface area and the exposure of active substances, leading to catalyst deactivation and a reduction in hydrogen production. The H_2 content increases from 11.63% at a 6% catalyst ratio to 27.49% at a 12% ratio (Table 8), indicating that low to moderate catalyst additions effectively promote H_2 generation. CO content also rises with increasing catalyst ratios, peaking at 20.82% at the 12% ratio. In contrast, CH_4 and CO_2 contents generally decrease with increasing catalyst ratios, likely because the catalyst facilitates further reactions, converting CH_4 and CO_2 into H_2 and CO. However, as the catalyst ratio increases further, the H_2 content declines, suggesting that the catalytic effect has reached saturation. Excessive catalyst may induce side reactions, ultimately reducing the H_2 yield. Considering this, the ratios of 8%, 10%, 12%, 14%, and 16% were selected for the optimization experiment.

3.3. Response Surface Experiment Results.

3.3.1. Model Variance Analysis. Variance analysis (ANOVA) assesses the variance of observed variables to identify which control variables have a significant impact. This method evaluates the effectiveness of models.[54] Table 9 presents the variance analysis for this model. Generally, a *p*-value less than 0.05 indicates that the corresponding factor is significant. Therefore, the quadratic polynomial model

https://doi.org/10.1021/acsomega.4c06104
ACS Omega 2024, 9, 44474−44486

Table 8. Gas Composition at Different Catalyst Addition Ratios

Catalyst addition ratio (%)[a]	H_2 (%)	CO (%)	CO_2 (%)	CH_4 (%)	C_xH_y (%)
6	11.63	12.75	37.44	19.12	19.06
8	13.86	14.45	35.67	17.74	18.28
10	18.92	17.31	31.83	15.44	16.50
12	27.49	20.82	25.71	13.16	12.82
14	27.14	20.93	27.06	14.38	10.49
16	26.85	21.78	28.42	12.35	10.60
18	25.94	19.65	26.54	13.76	14.11

[a]Conditions: conventional pyrolysis temperature of 450 °C and microwave irradiation time of 8 min.

Table 9. Variance Analysis for the Established Regression Model

Source	Sum of squares	Df	Mean squares	*F*-value	p-value
model	50.06	9	5.56	40.16	<0.0001
X_1	6.04	1	6.04	43.60	<0.0001
X_2	8.99	1	8.99	64.87	<0.0001
X_3	2.71	1	2.71	19.60	0.0017
X_1X_2	0.1225	1	0.1225	0.8845	0.3715
X_1X_3	0.0946	1	0.0946	0.6831	0.4299
X_2X_3	0.8646	1	0.8646	6.24	0.0339
X_1^2	10.82	1	10.82	78.12	<0.0001
X_2^2	21.47	1	21.47	155.02	<0.0001
X_3^2	14.21	1	14.21	102.61	<0.0001
residual	1.25	9	0.1385		
lack of fit	1.08	5	0.2153	5.06	0.0706
pure error	0.1701	4	0.0425		
cor total	51.31	18			
std. dev.	0.3722			R^2	0.9757

established in this experiment is highly significant ($p < 0.0001$).[55] The model's R^2 is 0.9757, and the adjusted R^2 is 0.9514, indicating a good fit with minimal experimental error. Thus, it can be used to analyze and predict UHP from the microwave pyrolysis of sludge.

Table 9 indicates that three factors in this model—conventional pyrolysis temperature, microwave irradiation time, and catalyst addition ratio—all have *p*-values less than 0.01, indicating their highly significant impact on UHP. The interaction between the latter two is significant ($p = 0.0339$), whereas the interactions between the former two factors, as well as between conventional pyrolysis temperature and catalyst addition ratio, are not. The quadratic terms of all three factors have *p*-values less than 0.05, indicating their significant effect on UHP.

$$y = -252.88 + 0.95X_1 + 4.06X_2 + 4.53X_3 + 0.0025X_1X_2 + 0.0022X_1X_3 - 0.0822X_2X_3 - 0.0011X_1^2 - 0.2381X_2^2 - 0.1937X_3^2 \quad (8)$$

By fitting the experimental data, regression eq 8 was established with UHP (y) as the dependent variable and conventional pyrolysis temperature (X_1), microwave irradiation time (X_2), and catalyst addition ratio (X_3) as independent variables.

Figure 8 compares the predicted and experimental values of UHP. Most experimental values are distributed around the predicted values, indicating that the selected model accurately

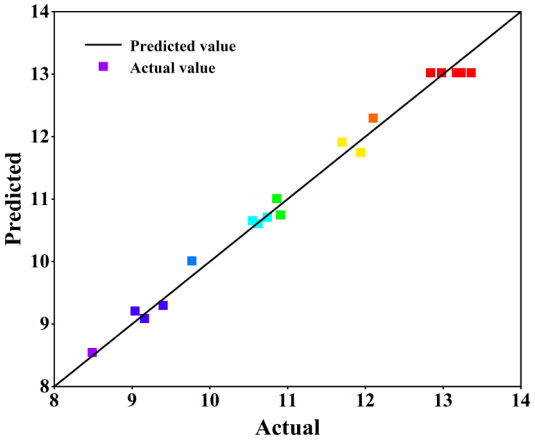

Figure 8. Predicted and actual values of UHP.

reflects the actual relationship between the independent and dependent variables. Therefore, this model is highly precise, allowing for accurate prediction of results.

3.3.2. Response Surface Analysis. Response surface plots visually represent the effects of two variables. A steeper slope indicates a greater effect of the independent variable on the response value, while a gentler slope indicates a smaller effect. An elliptical contour plot indicates significant interaction between two variables, whereas a near-circular contour plot suggests negligible interaction.[56] Three-dimensional response surface plots and contour plots were constructed from regression analysis results to study the interaction effects of the independent variables on UHP.

Figure 9a,b depicts the interaction between the conventional pyrolysis temperature and microwave irradiation time on UHP from sludge microwave pyrolysis. The UHP initially increased and then decreased with an increase in both factors. The longer the irradiation time, the more microwave energy the sludge absorbs. Under constant microwave power, this allows less time to reach the required pyrolysis temperature for hydrogen production. Moreover, due to the volumetric heating property of microwaves, heat can be generated throughout the entire volume of sludge.[57] Longer microwave irradiation time allows heat to be thoroughly transferred from the inside out, leading to more complete pyrolysis and higher hydrogen production. However, with further increases in microwave irradiation time, the pyrolysis temperature becomes excessively high, intensifying the reaction. As a result, some organic matter is carried out of the pyrolysis system by the generated gas before it has a chance to decompose, thereby reducing hydrogen production.

Increasing the conventional pyrolysis temperature can enhance the carbonization and ash content of sludge, thereby improving its dielectric properties and microwave absorption ability.[58] This enables the sludge under microwave irradiation to quickly reach a high pyrolysis temperature, determining the extent of the organic matter pyrolysis reaction within the sludge. Higher temperatures result in a more complete decomposition of organic matter. During pyrolysis, endothermic reactions occur, so higher temperatures favor the forward direction of the reaction, increasing gas volume and consequently producing more hydrogen.[59] However, as the temperature continues to increase, the initially pyrolyzed sludge shows a lower activation energy under microwave irradiation. This resulted in a faster reaction rate, a higher gas

https://doi.org/10.1021/acsomega.4c06104
ACS Omega 2024, 9, 44474−44486

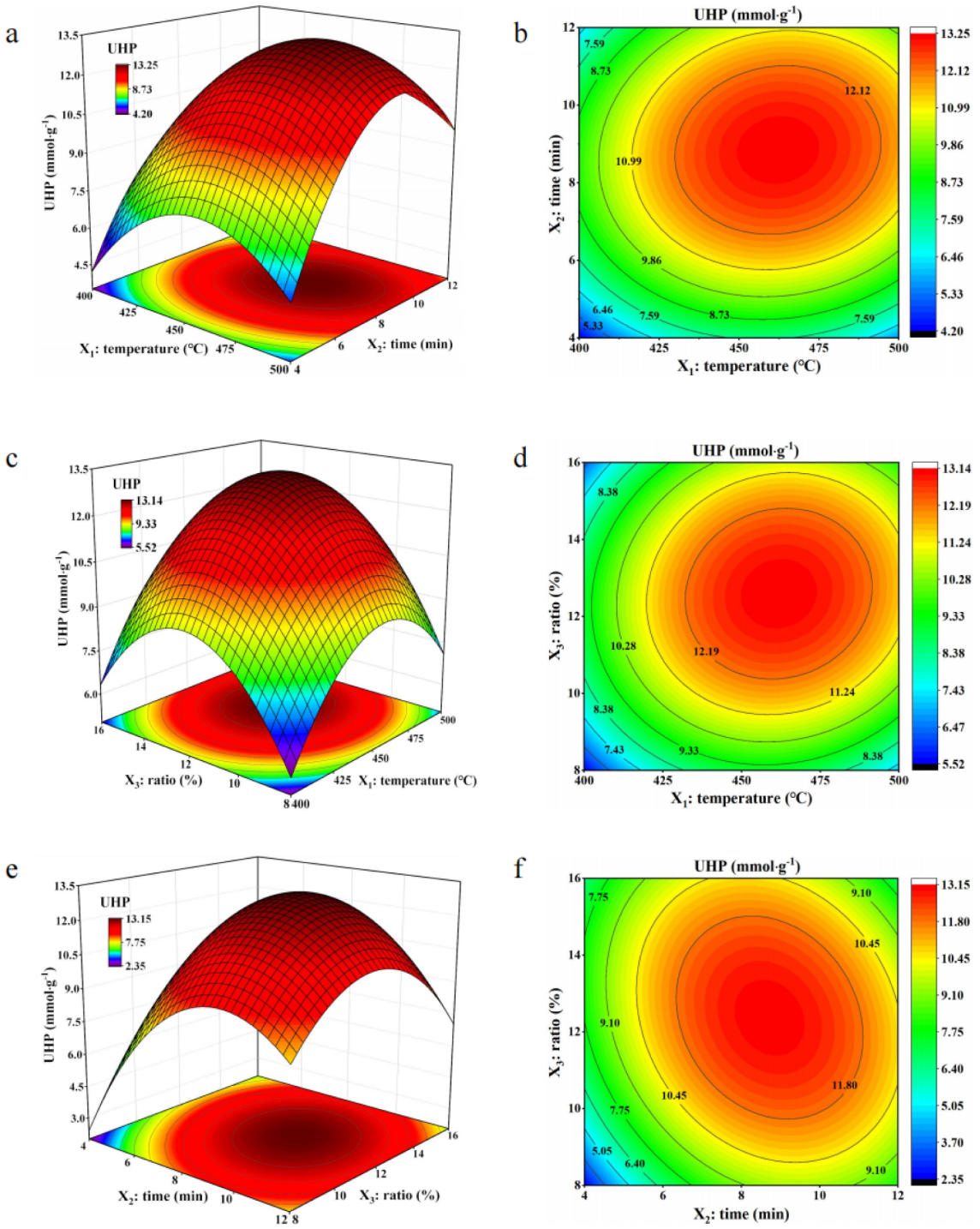

Figure 9. (a, c, e) Response surface and (b, d, f) respective contour plots for UHP.

release rate, and a shorter residence time in the reactor. Consequently, some organic matter and high-molecular compounds are carried away by the generated pyrolysis gas before they can decompose, reducing hydrogen production.[60]

Figure 9c,d illustrates the interaction between the conventional pyrolysis temperature and catalyst addition ratio on UHP from sludge microwave pyrolysis. Figure 9d demonstrates that when the microwave irradiation time is maintained at a central level, the UHP initially increases and then decreases with rising conventional pyrolysis temperature and catalyst addition ratio. At a conventional pyrolysis temperature between 425 and 475 °C and a catalyst addition ratio of 10−14%, the UHP is at a relatively high level. The active components in the SC-M catalyst are primarily Ni and Cu, which dissociates hydrocarbons by accepting electrons, thereby producing lighter products.[61] As the ratio increases, more metal active components become available. With a fixed sludge mass, more organic matter and tar can be catalytically cracked by active components, leading to greater hydrogen production from sludge pyrolysis at high temperatures. Additionally, influenced by the microwave electric field, Ni and Cu in the SC-M catalyst collide with organic matter in sludge,

https://doi.org/10.1021/acsomega.4c06104
ACS Omega 2024, 9, 44474−44486

accelerating chemical reactions, lowering reaction barriers, and forming microwave nonthermal effects.[62] An increased catalyst addition ratio (Ni and Cu contents) raises the frequency and range of collisions, breaking more C−H bonds in sludge. After the catalyst breaks, more H atoms migrate and collide within the catalyst, producing more hydrogen.

However, Figure 9c demonstrates that when the catalyst addition ratio exceeds 12%, UHP begins to gradually decrease. This may be because excessive catalyst content generates carbon during the reaction, which deposits on the surface, encapsulating the sludge and blocking the active centers and catalyst pores.[63] As a result, the sludge cannot be fully pyrolyzed, thus, reducing hydrogen production. According to the *F*-values in Table 9, the impact of conventional pyrolysis temperature (F = 43.60) is more significant than that of the catalyst addition ratio (F = 19.60).

Figure 9e,f illustrates the interaction effects of microwave irradiation time and catalyst addition ratio on UHP from sludge microwave pyrolysis. Figure 9e indicates that when the microwave irradiation time is between 4 and 8 min and the catalyst addition ratio is between 8% and 12%, the UHP gradually increases. However, when the irradiation time is between 8 and 12 min and the catalyst addition ratio is between 12% and 16%, the UHP gradually decreases. When the irradiation time is between 8 and 10 min and the catalyst addition ratio is between 12% and 14%, the UHP from sludge microwave pyrolysis is at a higher level. Figure 8f shows that the contour plot of the two factors is elliptical, indicating a significant interaction effect between them on UHP, as confirmed by the Prob > F value of 0.0339 for X_2X_3 in Table 9.

Additionally, Table 9 shows that the *F*-value for microwave irradiation time is 64.87, which is greater than the *F*-values for conventional pyrolysis temperature and catalyst addition ratio, indicating that it has the most significant effect on the UHP. The experiments revealed that sludge essentially completed pyrolysis within approximately 8−10 min of irradiation, which is faster than the estimated time. This could be related to the increased SC-M catalyst addition ratio, which accelerated the heating and pyrolysis rates. Consequently, the sludge reached the end point of microwave pyrolysis earlier, reducing energy consumption as well.[64]

3.4. Condition Optimization and Verification. Solving the regression fitting equation yields the optimal preparation conditions for UHP from sludge pyrolysis: a conventional pyrolysis temperature of 462.715 °C, a microwave irradiation time of 8.779 min, and a catalyst addition ratio of 12.438%. Under these conditions, the predicted UHP value is 13.37 mmol/g. Considering feasibility and practicality, the preparation conditions were adjusted to a conventional pyrolysis temperature of 462.7 °C, a microwave irradiation time of 8.8 min, and a catalyst addition ratio of 12.4%. To verify the accuracy of the predicted values, three parallel experiments were conducted under the adjusted conditions. The model showed that the predicted mean has a 95% probability of falling within the range of 12.42−13.63 mmol/g, while the actual measured mean was 13.22 mmol/g. The relative error between the actual measurement and the model prediction is only 1.12%, indicating that the preparation conditions for UHP from sludge microwave pyrolysis are accurate and reliable and have significant application value.

4. CONCLUSIONS

The SC-M catalyst was prepared from electroplating sludge by using carbonization and nitric acid modification methods. Characterization tests revealed that the catalyst had a specific surface area of 24.8 m^2/g and an average pore size of 14.68 nm. These properties indicate good active sites and pore structures, making it suitable for microwave catalytic pyrolysis experiments for hydrogen production from sludge.

Response surface optimization experiments showed that the quadratic regression model fit well. Variance analysis indicated that the effectiveness of the three factors on UHP was ranked as follows: microwave irradiation time > conventional pyrolysis temperature > catalyst addition ratio. Additionally, the interaction effect between the microwave irradiation time and catalyst addition ratio was significant.

The optimal conditions for the highest UHP, determined through response surface methodology optimization, were a conventional pyrolysis temperature of 462.7 °C, a microwave irradiation time of 8.8 min, and a catalyst addition ratio of 12.4%. Under these conditions, the experimental UHP was 13.22 mmol/g.

The results provide a theoretical foundation for process research on hydrogen production from sludge biomass via microwave pyrolysis and guide the comprehensive utilization of solid waste, such as sludge.

AUTHOR INFORMATION

Corresponding Author

Hailong Yu − *School of Petroleum and Natural Gas Engineering, School of Energy, Changzhou University, Changzhou 213164, China*; Email: yhl@cczu.edu.cn

Authors

Wenchang Qin − *School of Petroleum and Natural Gas Engineering, School of Energy, Changzhou University, Changzhou 213164, China*; orcid.org/0009-0004-5185-9541

Chaoqian Wang − *School of Petroleum and Natural Gas Engineering, School of Energy, Changzhou University, Changzhou 213164, China*

Shuting Qin − *School of Petroleum and Natural Gas Engineering, School of Energy, Changzhou University, Changzhou 213164, China*

Xiaolong Li − *School of Petroleum and Natural Gas Engineering, School of Energy, Changzhou University, Changzhou 213164, China*

Complete contact information is available at: https://pubs.acs.org/10.1021/acsomega.4c06104

Notes

The authors declare no competing financial interest.

ACKNOWLEDGMENTS

This study was supported by the Jiangsu Province Graduate Research and Innovation Plan (Project No.: SJCX23_1575, SJCX24_1694).

REFERENCES

(1) Zou, C.; Li, J.; Zhang, X.; Jin, X.; Xiong, B.; Yu, H.; Liu, X.; Wang, S.; Li, Y.; Zhang, L.; Miao, S.; Zheng, D.; Zhou, H.; Song, J.; Pan, S. Industrial status, technological progress, challenges and prospects of hydrogen energy. *Nat. Gas Ind.* **2022**, *9*, 427−447.

https://doi.org/10.1021/acsomega.4c06104
ACS Omega 2024, 9, 44474−44486

(2) Meng, G.; Zhao, B.; Zhang, X.; Chen, L.; Xu, H.; Sun, L. Study on hydrogen production from biomass by twice decomposition. *Acta Energiae Solaris Sinica* **2009**, *30*, 837−841.
(3) Racek, J.; Sevcik, J.; Chorazy, T.; Kucerik, J.; Hlavinek, P. Biochar−Recovery Material from Pyrolysis of Sewage Sludge: A Review. *Waste Biomass Valor.* **2020**, *11*, 3677−3709.
(4) Wang, F.; Wang, J.; Yu, Z.; Ma, J.; Liu, L.; Wang, T.; Guo, H. Obtaining High Yield Hydrogen from Sewage Sludge by Two-Stage Gasification: Alkaline Pyrolysis Coupled with Catalytic Reforming. *ACS Omega* **2022**, *7*, 22192−22198.
(5) Guo, S.; Wang, H.; Liu, X.; Zhang, Z.; Liu, Y. Approaches for the Treatment and Resource Utilization of Electroplating Sludge. *Materials* **2024**, *17*, 1707.
(6) Cao, C.; Yu, J.; Xu, J.; Li, F.; Yang, Z.; Wang, G.; Zhang, S.; Cheng, Z.; Li, T.; Pu, Y.; Xian, J.; Yang, Y.; Pu, Z. A review on fabricating functional materials by electroplating sludge: process characteristics and outlook. *Environ. Sci. Pollut. Res.* **2023**, *30*, 64827−64844.
(7) Tian, L.; Chen, L.; Gong, A.; Wu, X.; Cao, C.; Liu, D.; Chen, Z.; Xu, Z.; Liu, Y. Separation and Extraction of Valuable Metals from Electroplating Sludge by Carbothermal Reduction and Low-Carbon Reduction Refining. *JOM* **2020**, *72*, 782−789.
(8) Li, T.; Wei, G.; Liu, H.; Gong, Y.; Zhao, H.; Wang, Y.; Wang, J. Comparative study of electroplating sludge reutilization in China: environmental and economic performances. *Environ. Sci. Pollut. Res.* **2023**, *30*, 106598−106610.
(9) Wang, H.; Liu, X.; Zhang, Z. Approaches for electroplating sludge treatment and disposal technology: Reduction, pretreatment and reuse. *J. Environ. Manag.* **2024**, *349*, 119535.
(10) Chang, H.; Zhao, Y.; Bisinella, V.; Damgaard, A.; Christensen, T. H. Climate change impacts of conventional sewage sludge treatment and disposal. *Water Res.* **2023**, *240*, 120109.
(11) Vishwajith, A. G.; Mahanama, K. R.; Wijesinghe, L. P. Investigation on the effective disposal of sludge from a water treatment plant. *Water Pract. Technol.* **2023**, *18*, 130−139.
(12) Niu, S.; Chen, M.; Li, Y.; Song, J. Co-combustion characteristics of municipal sewage sludge and bituminous coal. *J. Therm. Anal. Calorim.* **2018**, *131*, 1821−1834.
(13) Li, H. *Research Progress on Comprehensive Utilization of Municipal Sludge*; China Resources Comprehensive Utilization: 2022, 104−106.
(14) Han, L.; Li, J.; Qu, C.; Shao, Z.; Yu, T.; Yang, B. Recent Progress in Sludge Co-Pyrolysis Technology. *Sustainability* **2022**, *14*, 7574.
(15) Li, H.; Xu, J.; Nyambura, S. M.; Wang, J.; Li, C.; Zhu, X.; Feng, X.; Wang, Y. Food waste pyrolysis by traditional heating and microwave heating: A review. *Fuel* **2022**, *324*, 124574.
(16) Zhang, S.; Qiu, Q.; Zeng, C.; Paik, K. W.; He, P.; Zhang, S. A review on heating mechanism, materials and heating parameters of microwave hybrid heated joining technique. *J. Manuf Process* **2024**, *116*, 176−191.
(17) Arpia, A. A.; Chen, W.-H.; Lam, S. S.; Rousset, P.; De Luna, M. D. G. Sustainable biofuel and bioenergy production from biomass waste residues using microwave-assisted heating: A comprehensive review. *Chem. Eng. J.* **2021**, *403*, 126233.
(18) Moseley, J. D.; Woodman, E. K. Energy Efficiency of Microwave-and Conventionally Heated Reactors Compared at meso Scale for Organic Reactions. *Energy Fuels* **2009**, *23*, 5438−5447.
(19) Domínguez, A.; Menéndez, J. A.; Inguanzo, M.; Píss, J. J. Production of bio-fuels by high temperature pyrolysis of sewage sludge using conventional and microwave heating. *Bioresour. Technol.* **2006**, *97* (10), 1185−1193.
(20) Domínguez, A.; Fernández, Y.; Fidalgo, B.; Pis, J. J.; Menéndez, J. A. Bio-syngas production with low concentrations of CO_2 and CH_4 from microwave-induced pyrolysis of wet and dried sewage sludge. *Chemosphere* **2008**, *70*, 397−403.
(21) Liu, L.; Zhang, J.; Wu, X.; Tian, Y. Production of biosyngas from continuous microwave-induced pyrolysis of sewage sludge. *Chin. J. Environ. Eng.* **2016**, *10*, 6622−6628.
(22) Deng, W.; Liu, S.; Ma, J.; Su, Y. Microwave-assisted ethanol decomposition over pyrolysis residue of sewage sludge for hydrogen-rich gas production. *Int. J. Hydrogen Energy* **2018**, *43*, 15762−15772.
(23) Fuentes-Cano, D.; Salinero, J.; Haro, P.; Nilsson, S.; Gómez-Barea, A. The influence of volatiles to carrier gas ratio on gas and tar yields during fluidized bed pyrolysis tests. *Fuel* **2018**, *226*, 81−86.
(24) Ma, R.; Sun, S.; Geng, H.; Fang, L.; Zhang, P.; Zhang, X. Study on the characteristics of microwave pyrolysis of high-ash sludge, including the products, yields, and energy recovery efficiencies. *Energy* **2018**, *144*, 515−525.
(25) Yu, Y.; Yu, J.; Yan, Z. Rapid pyrolysis of sewage sludge for the production of bio-oil and syngas under microwave radiation. *Environ. Chem.* **2013**, *32*, 486−491.
(26) Wang, T.; Hu, J.; Xia, L.; Qu, X. Microwave pyrolysis of sewage sludge and analysis on the structure and components of pyrolysis products. *Journal Of Shenyang Jianzhu University(natural Science)* **2008**, *30*, 662−666.
(27) Sun, J.; Jiang, Z.; Wang, K.; Li, F.; Song, Z.; Wang, W.; Zhao, X.; Mao, Y. Experimental Study on Microwave−SiC-Assisted Catalytic Hydrogenation of Phenol. *Energy Fuels* **2019**, *33*, 11092−11100.
(28) Lin, Q.; Chen, G.; Liu, Y. Scale-up of microwave heating process for the production of bio-oil from sewage sludge. *J. Anal. Appl. Pyrol.* **2012**, *94*, 114−119.
(29) Chen, H.; Zuo, W.; Zhang, J.; Wu, X.; Gong, Z.; Tian, Y. Impact of nickel-based catalyst on biosyngas performance produced by microwave-induced catalytic pyrolysis of sludge. *Chin. J. Environ. Eng.* **2014**, *8*, 1150−1156.
(30) Chen, G.; Hu, M.; Du, G.; Tian, S.; He, Z.; Liu, B.; Ma, W. Hydrothermal Liquefaction of Sewage Sludge by Microwave Pretreatment. *Energy Fuels* **2020**, *34*, 1145−1152.
(31) Yang, B.; Dai, J.; Zhao, Y.; Wu, J.; Ji, C.; Zhang, Y. Advances in preparation, application in contaminant removal, and environmental risks of biochar-based catalysts: a review. *Biochar* **2022**, *4* (1), 51.
(32) An, Y.; Tahmasebi, A.; Zhao, X.; Matamba, T.; Yu, J. Catalytic reforming of palm kernel shell microwave pyrolysis vapors over iron-loaded activated carbon: enhanced production of phenol and hydrogen. *Bioresour. Technol.* **2020**, *306*, 123111.
(33) Dong, Q.; Niu, M.; Bi, D.; Liu, W.; Gu, X.; Lu, C. Microwave-assisted catalytic pyrolysis of moso bamboo for high syngas production. *Bioresour. Technol.* **2018**, *256*, 145−151.
(34) Liu, Q.; Zhou, H.; Jia, Z. Hydrogen Production by Ethanol Reforming on Supported Ni−Cu Catalysts. *ACS Omega* **2022**, *7* (5), 4577−4584.
(35) Hong, C.; Haiyun, W. Optimization of volatile fatty acid production with co-substrate of food wastes and dewatered excess sludge using response surface methodology. *Bioresour. Technol.* **2010**, *101*, 5487−5493.
(36) Wang, J.; Wan, W. Experimental design methods for fermentative hydrogen production: A review. *Int. J. Hydrogen Energy* **2009**, *34*, 235−244.
(37) Zhang, P.; Liu, C.; Zheng, Y.; Zhao, Y.; Zhen, G. Statistical Key Factor Optimization of Conditions for Biohydrogen Production from Sewage Sludge and Food Waste by Anaerobic Codigestion. *Energy Fuels* **2019**, *33*, 11163−11172.
(38) Wang, C.; Zhang, X.; Wang, W.; Sun, J.; Mao, Y.; Zhao, X.; Song, Z. A stepwise microwave synergistic pyrolysis approach to produce sludge-based biochars: Optimizing and mechanism of heavy metals immobilization. *Fuel* **2022**, *314*, 122770.
(39) Zhang, L.; An, L.; Wei, H.; Yin, J.; Li, H. Treatment of m-cresol wastewater by catalytic oxidation with modifing sludge carbon. *Environ. Prot. Chem. Ind.* **2022**, *42*, 268−273.
(40) Yue, Y.; Niu, P.; Jiang, L.; Cao, Y.; Bao, X. Acid-Modified Natural Bauxite Mineral as a Cost-Effective and High-Efficient Catalyst Support for Slurry-Phase Hydrocracking of High-Temperature Coal Tar. *Energy Fuels* **2016**, *30*, 9203−9209.
(41) Ghafarzadeh, M.; Abedini, R.; Rajabi, R. Optimization of ultrasonic waves application in municipal wastewater sludge treatment using response surface method. *J. Cleaner Prod.* **2017**, *150*, 361−370.

https://doi.org/10.1021/acsomega.4c06104
ACS Omega 2024, 9, 44474−44486

(42) Jiaxin, W.; Jiao, H.; Xue, L.; Yue, X.; Caishun, Z.; Daosheng, L.; Xiaoning, H.; Yajie, L.; Lei, Z.; Zhixian, G. Preparation and properties of MnCu/Ce cataiyst for CO preferential oxidation reaction. *J. Fuel Chem. Technol.* **2024**, *52*, 565−576.
(43) Sun, L.; Deng, Q.; Li, Y.; Mi, H.; Wang, S.; Deng, L.; Ren, X.; Zhang, P. CoO-Co_3O_4 heterostructure nanoribbon/RGO sandwich-like composites as anode materials for high performance lithium-ion batteries. *Electrochim. Acta* **2017**, *241*, 252−260.
(44) Chen, H.; Gao, Y.; Ye, L.; Yao, Y.; Chen, X.; Wei, Y.; Sun, L. A Cu 2 Se−Cu 2 O film electrodeposited on titanium foil as a highly active and stable electrocatalyst for the oxygen evolution reaction. *Chem. Commun.* **2018**, *54* (39), 4979−4982.
(45) Lv, Y.; Shi, B.; Qi, Y.; Su, X.; Liu, L.; Tian, L.; Ding, J. Synthesis and characterization of the maize-leaf like Cu_2O nanosheets array film via an anodic oxidation method. *J. Alloys Compd.* **2019**, *773*, 706−712.
(46) Lv, H.; Sun, H. Electrospun Foamlike NiO/CuO Nanocomposites with Superior Catalytic Activity toward the Reduction of 4-Nitrophenol. *ACS Omega* **2020**, *5*, 11324−11332.
(47) Wu, N.; Wu, B.; Xu, Y.; Tang, X. Relationships of the Degree of C = C Double Bond Conversion with the Dielectric Properties for SiO_2/1,2-PB/SBS/EPDM Composites Cured by Organic Peroxide. *ChemistrySelect* **2022**, *7* (3), No. e202104078.
(48) Davari, F.; Fadavieslam, M. R. The effect of copper doping on the structural, optical, and electrical properties of cadmium oxide thin films deposited by the spray pyrolysis technique. *Indian J. Phys.* **2023**, *97*, 2977−2989.
(49) Vajpayee, M.; Singh, M.; Ledwani, L.; Prakash, R.; Nema, S. K. Investigation of Antimicrobial Activity of DBD Air Plasma-Treated Banana Fabric Coated with Natural Leaf Extracts. *ACS Omega* **2020**, *5*, 19034−19049.
(50) Xing, W.; Liu, Y.; Zhang, W.; Sun, Y.; Kai, X.; Yang, T. Study on Methanation Performance of Biomass Gasification Syngas Based on a Ni/Al_2O_3 Monolithic Catalyst. *ACS Omega* **2020**, *5*, 28597−28605.
(51) Chen, G. B.; Wu, F. H.; Fang, T. L.; Lin, H. T.; Chao, Y. C. A study of Co-gasification of sewage sludge and palm kernel shells. *Energy* **2021**, *218*, 119532.
(52) Jokar, R.; Jahromi, H.; Bhattrai, A.; Adhikari, S. Biocarbon-catalyzed methane decomposition towards clean hydrogen and enhanced biocarbon production. *Int. J. Hydrogen Energy* **2024**, *70*, 105−117.
(53) Xie, Q.; Chen, Z.; Zhou, Y.; Pan, T.; Duan, Y.; Yu, S.; Liang, X.; Wu, Z.; Ji, W.; Nie, Y. Efficient Treatment of Oily Sludge via Fast Microwave-Assisted Pyrolysis, Followed by Thermal Plasma Vitrification. *Molecules* **2023**, *28*, 4036.
(54) Huang, X.; Lv, Z.; Zhao, B.; Zhang, H.; Yao, X.; Shuai, Y. Optimization of operating parameters for methane steam reforming thermochemical process using Response Surface Methodology. *Int. J. Hydrogen Energy* **2022**, *47*, 28313−28321.
(55) Chollom, M. N.; Rathilal, S.; Swalaha, F. M.; Bakare, B. F.; Tetteh, E. K. Comparison of response surface methods for the optimization of an upflow anaerobic sludge blanket for the treatment of slaughterhouse wastewater. *Environ. Eng. Res.* **2020**, *25*, 114−122.
(56) Hosseinpour, M.; Soltani, M.; Noofeli, A.; Nathwani, J. An optimization study on heavy oil upgrading in supercritical water through the response surface methodology (RSM). *Fuel* **2020**, *271*, 117618.
(57) Lin, B.; Cao, X.; Liu, T.; Ni, Z.; Wang, Z. Experimental Research on Water Migration-Damage Characteristics of Lignite under Microwave Heating. *Energy Fuels* **2021**, *35*, 1058−1069.
(58) Wang, C.; Wang, W.; Lin, L.; Zhang, F.; Zhang, R.; Sun, J.; Song, Z.; Mao, Y.; Zhao, X. A stepwise microwave synergistic pyrolysis approach to produce sludge-based biochars: Feasibility study simulated by laboratory experiments. *Fuel* **2020**, *272*, 117628.
(59) Ren, L.; Zhang, K.; Zhang, Y.; Wang, F.; Yang, F.; Cheng, F. Mechanism of gas production under microwave/conventional pyrolysis of sewage sludge: Mechanism of microwave energy action on oxygen-containing functional groups. *Chem. Eng. J.* **2023**, *464*, 142511.
(60) Deng, W.; Su, Y.; Liu, S.; Shen, H. Microwave-assisted methane decomposition over pyrolysis residue of sewage sludge for hydrogen production. *Int. J. Hydrogen Energy* **2014**, *39*, 9169−9179.
(61) Luo, J.; Gong, G.; Ma, R.; Sun, S.; Cui, C.; Cui, H.; Sun, J.; Ma, N. Study on high-value products of waste plastics from microwave catalytic pyrolysis: Construction and performance evaluation of advanced microwave absorption-catalytic bifunctional catalysts. *Fuel* **2023**, *346*, 128296.
(62) Rao, B.; Su, J.; Xu, S.; Pang, H.; Xu, P.; Zhang, Y.; Zhu, J.; Tu, H. Thermal and non-thermal mechanism of microwave irradiation on moisture content reduction of municipal sludge. *Water Res.* **2022**, *226*, 119231.
(63) Wang, B.; Liu, Y.; Guan, Y.; Zhang, G.; Xing, D. Hydrogen production and coke resistance characteristic during volatile reforming over Fe_2O_3−Ce_2O_3/sludge char catalyst. *J. Cleaner Prod.* **2024**, *434*, 139836.
(64) Oh, D. Y.; Kim, D.; Choi, H.; Park, K. Y. Syngas generation from different types of sewage sludge using microwave-assisted pyrolysis with silicon carbide as the absorbent. *Heliyon* **2023**, *9*, No. e14165.

https://doi.org/10.1021/acsomega.4c06104
ACS Omega 2024, 9, 44474−44486